

## **DYNAMIC RESPONSE OF A POROELASTIC SOIL MEDIUM TO A MOVING LOAD ON ITS SURFACE**

**D.D. THEODORAKOPOULOS<sup>1</sup>, D. E. BESKOS<sup>2</sup>**

### **ABSTRACT**

The problem of the determination of the dynamic response of a fully saturated poroelastic soil stratum on bedrock to a moving load with constant velocity is studied analytically- numerically under conditions of plane strain. The applied load is considered to be the sum of a large number of harmonics with varying frequency in the form of a Fourier expansion. Two methods of solution are employed: an “exact” direct method which solves the governing partial differential equations of the problem by separation of variables and an approximate method of solution, which considers the total field to be the result of the superposition of an elastodynamic problem with modified elastic constants and mass density for the whole domain and a diffusion problem for the pore fluid pressure confined to a boundary layer near the free surface of the medium, which are solved analytically in the frequency domain. Both methods provide soil displacements and stresses as well as pore water pressures in an explicit form. Numerical evaluation of those expressions permit one to find the dynamic response for various values of the shear modulus, compressibility of fluid, porosity, permeability and load speed. Thus, a detailed assessment of the relative importance of those parameters on the response can be accomplished. In addition, one can also determine the range of the material and load parameters for which the approximate but simpler solution can lead to satisfactory results.

### **INTRODUCTION**

The study of the dynamic behavior of a half-space soil medium under the action of moving loads on its free surface is fundamental to the design of structures in the area of geotechnical / transportation facilities and has thus received a great attention over the past decades. The available methods of the dynamic analysis of the soil medium due to moving loads can be grouped into three categories (Theodorakopoulos 2003) depending mainly on the degree of modeling elaboration of the soil material.

In the present work, the dynamic response of a uniform, fully saturated poroelastic layer of soil under the action of a strip load moving at constant velocity is obtained analytically under conditions of plane strain. Hysteretic damping in the soil skeleton may also be present. The dynamic poroelastic theory of Biot (1956) with the notation of Mei and Foda (1981) is employed in this work.

The exact analytical solution of the above problem was found to be rather complicated. In an effort to obtain an approximate analytical solution of the same problem, characterized by simplicity and satisfactory accuracy, the superposition method of Mei and Foda (1981) was also employed in this paper. According to this method, the total field of a poroelastodynamic problem obeying Biot's (1956)

---

<sup>1</sup> Professor, Department of Civil Engineering, University of Patras, Greece, Email: [d.d.theod@upatras.gr](mailto:d.d.theod@upatras.gr)

<sup>2</sup> Professor, Department of Civil Engineering, University of Patras, Greece, Email: [d.e.beskos@upatras.gr](mailto:d.e.beskos@upatras.gr)

theory can be approximated by the superposition of i) an elastodynamic problem with modified elastic constants and mass density for the whole domain (outer approximation) and ii) a diffusion problem for the pore fluid pressure confined to a boundary layer at the free surface of the domain (boundary layer correction).

The distributed load, which moves at constant velocity, is expanded in Fourier series as in Theodorakopoulos et al (2003). The exact solution as well as the outer approximation and the boundary layer correction are all obtained analytically/ numerically. The results of the approximate method are compared against those of the exact one in order to establish the range of the various parameters of the problem for which the accuracy of this approximate method is satisfactory.

## EXACT APPROACH

### Governing equations of motion

Consider a soil system consisting of an infinite, uniform layer of a porous elastic solid material saturated by a viscous fluid of height  $H$ , bonded to a rigid base. At the free upper surface of the medium a strip load moves at a constant velocity  $c$ . Material damping for the solid skeleton,  $\delta$ , is considered to be of hysteretic type. A cross-section of this system along the  $(x, z)$  plane is shown in Figure 1. Assuming plane strain conditions, the equations of dynamic poroelasticity due to Biot (1956) can be written in the form (Theodorakopoulos, 2003)

$$(\lambda^* + 2G^*) \frac{\partial^2 u}{\partial x^2} + (\lambda^* + G^*) \frac{\partial^2 w}{\partial x \partial z} + G^* \frac{\partial^2 u}{\partial z^2} - \frac{\partial p}{\partial x} = (1-f) \rho_s \ddot{u} + f \rho_f \ddot{u}^f \quad (1)$$

$$(\lambda^* + 2G^*) \frac{\partial^2 w}{\partial z^2} + (\lambda^* + G^*) \frac{\partial^2 u}{\partial x \partial z} + G^* \frac{\partial^2 w}{\partial x^2} - \frac{\partial p}{\partial z} = (1-f) \rho_s \ddot{w} + f \rho_f \ddot{w}^f \quad (2)$$

$$k \left( \frac{\partial^2 p}{\partial x^2} + \frac{\partial^2 p}{\partial z^2} \right) - \frac{f}{\beta} \dot{p} - \frac{k p_f}{\beta} \ddot{p} = \left( \frac{\partial \dot{u}}{\partial x} + \frac{\partial \dot{w}}{\partial z} \right) - k p_f \frac{f-1}{f} \left( \frac{\partial \ddot{u}}{\partial x} + \frac{\partial \ddot{w}}{\partial z} \right) \quad (3)$$

$$-\frac{f^2}{k} (\dot{u}^f - \dot{u}) - f \frac{\partial p}{\partial x} = f \rho_f \ddot{u}^f \quad (4)$$

$$-\frac{f^2}{k} (\dot{w}^f - \dot{w}) - f \frac{\partial p}{\partial z} = f \rho_f \ddot{w}^f \quad (5)$$

where  $p$  = the pore water pressure,  $u$  and  $w$  = the  $x$  and  $z$  displacement components, respectively, of the solid relative to the rigid base, and  $u^f$  and  $w^f$  = the corresponding relative displacement components of the fluid. Furthermore,  $f$  = the porosity,  $\rho_s$  and  $\rho_f$  = the actual mass densities of the solid and fluid, respectively,  $k$  = the coefficient of permeability,  $\beta$  = the bulk modulus of the fully saturating fluid,  $G^*$  and  $\lambda^*$  = the complex-valued Lamé elastic constants given by  $G^* = G(1 + \delta)$  and  $\lambda^* = G^* 2\nu / (1 - 2\nu)$ , respectively, with  $\nu$  = the Poisson's ratio.

### Moving load representation

The applied load configuration is shown in Figure 1 and details of its Fourier series expansion can be found in Theodorakopoulos (2003). Thus, one can write

$$F(x - ct) = \text{Re} \sum_{n=0}^{2048} F_n e^{i\lambda_n(x-ct)} \quad (6)$$

in which

$$\lambda_n = n \frac{\pi}{L}$$

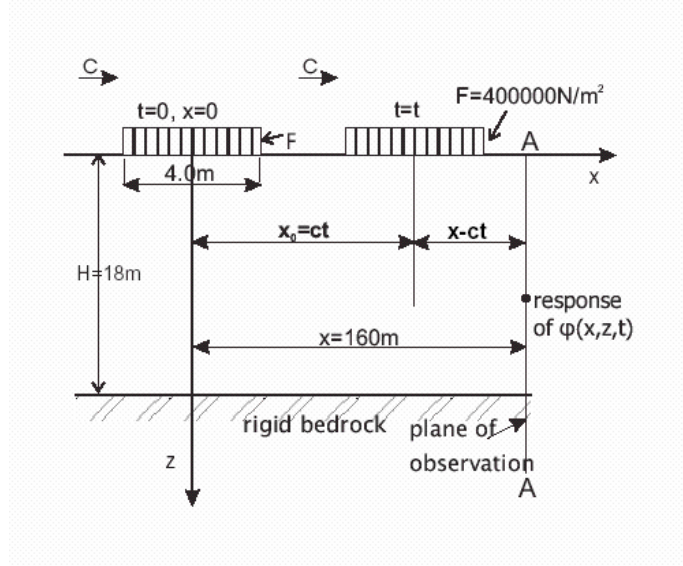


Figure 1. Configuration of traveling surface load and plane of observation

$$F_n = \begin{cases} \frac{\ell}{L} F & \text{for } n = 0 \\ 2 \frac{1}{n\pi} \sin\left(n\pi \frac{\ell}{L}\right) F & \text{for } n > 0 \end{cases} \quad (7)$$

where  $2\ell$  = the width of the strip load and  $2L$  = the wave length.

#### Solution of the governing equations

Assuming for every response function  $\phi(x, z, t)$  the form

$$\phi(x, z, t) = \text{Re} \sum_{n=0}^{2048} \Phi_n(z) e^{i\lambda_n(x-ct)} \quad (8)$$

in which the dependence on  $x$  is only represented in the exponential function and the dependence on  $z$  in the function  $\Phi_n(z) = \Phi_n$  for the  $n^{\text{th}}$  harmonic, one can finally derive the following governing equations:

$$a_1 W_n'' + b_1 W_n + c_1 P_n' + d_1 U_n' = 0 \quad (9)$$

$$a_2 U_n'' + b_2 U_n + c_2 P_n + d_2 W_n' = 0 \quad (10)$$

$$a_3 P_n'' + b_3 P_n + c_3 W_n' + d_3 U_n = 0 \quad (11)$$

where primes indicate differentiation with respect to  $z$  and the coefficients  $a_1, b_1, c_1, d_1, a_2, b_2, c_2, d_2, a_3, b_3, c_3$  and  $d_3$  can be found elsewhere (Theodorakopoulos 2003). The solution of Eqs (9)-(11) is given by

$$W_n = \sum_{\kappa=1}^6 A_{\kappa n} e^{q_{\kappa} z}, U_n = \sum_{\kappa=1}^6 \mu_{\kappa} r_{\kappa} A_{\kappa n} e^{q_{\kappa} z}, P_n = \sum_{\kappa=1}^6 r_{\kappa} A_{\kappa n} e^{q_{\kappa} z} \quad (12)$$

in which the integration constants  $A_{\kappa n}$ ,  $\mu_{\kappa} r_{\kappa} A_{\kappa n}$  and  $r_{\kappa} A_{\kappa n}$  may now be determined by employing the boundary conditions:

$$\text{At bottom } (z = H): u = 0, w = 0, \frac{\partial p}{\partial z} = 0 \quad (13)$$

$$\text{At surface } (z = 0): \tau_{xz} = 0, \tau_z = F, p = 0 \quad (14)$$

These constants and the coefficients  $q_{\kappa}$  can be found in Theodorakopoulos (2003). Thus, finally, with the use of the general expressions (8), the solid displacements and pore pressure can be written in the form

$$w(x, z, t) = Re \sum_{n=-\infty}^{\infty} \left( \sum_{\kappa=1}^6 A_{\kappa n} e^{q_{\kappa} z} \right) e^{i\lambda_n(x-ct)} \quad (15)$$

$$u(x, z, t) = Re \sum_{n=-\infty}^{\infty} \left( \sum_{\kappa=1}^6 \mu_{\kappa} r_{\kappa} A_{\kappa n} e^{q_{\kappa} z} \right) e^{i\lambda_n(x-ct)} \quad (16)$$

$$p(x, z, t) = Re \sum_{n=-\infty}^{\infty} \left( \sum_{\kappa=1}^6 r_{\kappa} A_{\kappa n} e^{q_{\kappa} z} \right) e^{i\lambda_n(x-ct)} \quad (17)$$

Furthermore, the expression for the effective vertical stress of solid is given by

$$\tau_z(x, z, t) = Re \sum_{n=-\infty}^{\infty} T_{z,n}(z) e^{i\lambda_n(x-ct)} \quad (18.a)$$

where, from the expression

$\tau_z = (\lambda^* + 2G^*) \partial w / \partial z + \lambda^* \partial u / \partial x$ , one has

$$T_{z,n}(z) = (\lambda^* + 2G^*) W_n'(z) + \lambda^* U_n(z) \lambda_n i \quad (18.b)$$

### Numerical results and discussion

The numerical results of this section have been obtained for the case of a single poroelastic infinite layer of depth 18m rested on an impervious bedrock. The surface of the layer is subject to a discretized moving strip load of constant intensity  $F=400.000 \text{ N/m}^2$ , of width  $2\ell=4.0\text{m}$  and  $2L = 409.6\text{m}$ . The main physical quantities of interest in this work are the vertical displacement of solid  $w(x, z, t)$ , the pore water pressure  $p(x, z, t)$  and the solid vertical effective stress  $\tau_z(x, z, t)$  for which the full results can be found in Theodorakopoulos (2003). In what follows, the time  $t=0$  corresponds to the instant at which the center of the applied load passes the point with  $x=0$  and  $z=0$ . Furthermore, it is clear that any response pattern underneath the load, at any time  $t$ , will appear to be the same for an observer travelling with velocity  $c$ . Figure 2 shows the vertical distribution of the maximum vertical displacement for an incompressible fluid ( $\beta = \infty$ ) and  $c=20\text{m/s}$  (72 km/h) for various values of shear modulus. It can be seen that the displacement response increases with decreasing values of  $G$ , as expected, since a softer solid shares a smaller portion of the applied load. The effect of the load velocity  $c$  on the vertical displacement is shown in Figure 3 for  $\beta = 2.45 \times 10^9 \text{ N/m}^2$  (compressibility of pure water for full saturation) and for two values of porosity  $f$ . One can see that for

$G=10^8 \text{ N/m}^2$  (hard solid material) the displacement response is not sensitive to any change of porosity even for high values of velocity,  $c=100\text{m/s}$  (360 km/h). However, as found in Theodorakopoulos (2003), in a softer medium with  $G$  say  $0.2 \times 10^8 \text{ N/m}^2$ , the effect of increasing values of porosity and permeability on the response is apparent in the range of high speeds, where load velocity greater than  $90\text{m/s}$  approaches that of the Rayleigh wave, which is the dominant contributor to the response in a region near the surface.

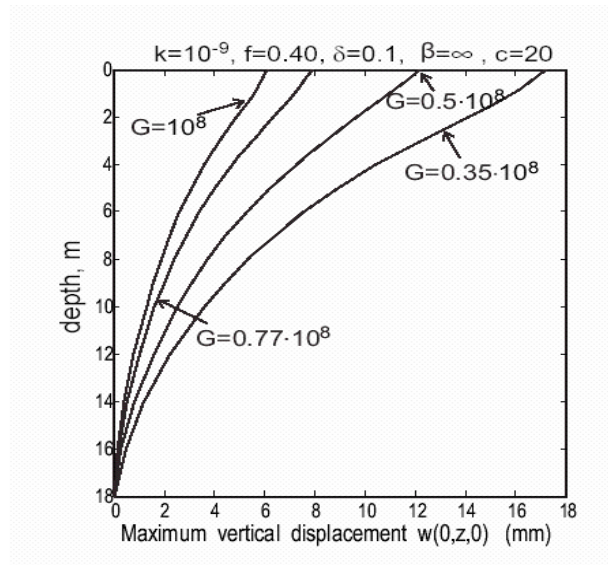


**Figure 2. Effect of shear modulus on maximum solid vertical displacement versus depth: poroelastic case**

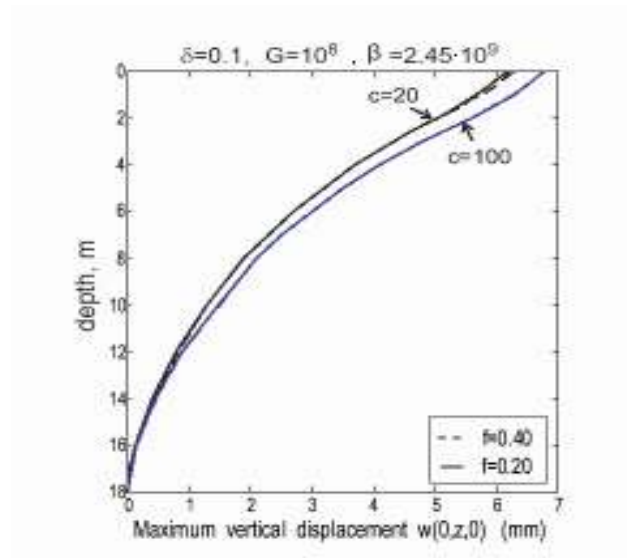


**Figure 3. Profile of maximum solid vertical displacement with depth for two values of porosity:  $k = 10^{-9} \text{ m}^3/\text{s}/\text{kg}$**

Figures 4 (a) and (b) show the vertical variation of the pore water pressure  $p$  for two values of porosity, two values of velocity  $c$  and a specific value of permeability in each figure. It can be seen that near the free surface the porewater pressure increases with decreasing permeability for both values of velocity, suggesting a destabilizing trend at the upper soil region. Furthermore, for a fine material ( $k = 10^{-9} \text{ m}^3/\text{s}/\text{kg} = 10^{-5} \text{ m/s}$ ) the pore pressure diminishes rapidly with depth to a nearly constant value

after its maximum value near the surface has been attained. For a coarse material ( $k = 10^{-7} \text{ m}^3/\text{s/kg} = 10^{-3} \text{ m/s}$ ) the variation of  $p$  with depth is more gradual for high velocities and constant for low velocities after its maximum value has been reached. It should be mentioned here that the porewater pressure distribution in Figures 4 (a) – (b) is similar to the one given in Foda et al (1983) for the case of Rayleigh waves in a poroelastic half space.

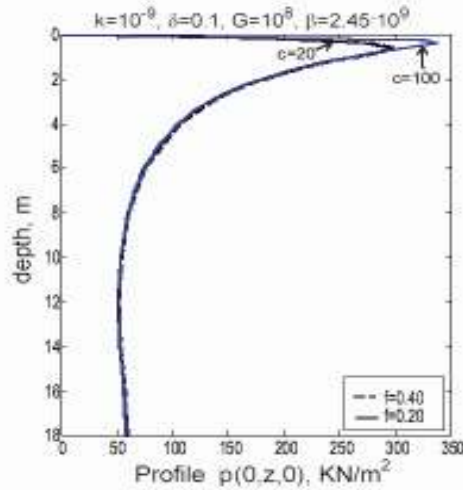


**Figure 4(a). Profile of porewater pressure with depth for various values of porosity:  $k = 10^{-9} \text{ m}^3/\text{s/kg}$ ,  $G = 10^8 \text{ N/m}^2$**

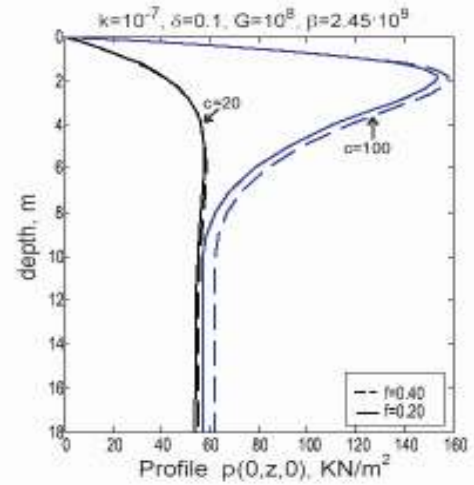


**Figure 4(b). Profile of porewater pressure with depth for various values of porosity:  $k = 10^{-7} \text{ m}^3/\text{s/kg}$ ,  $G = 10^8 \text{ N/m}^2$**

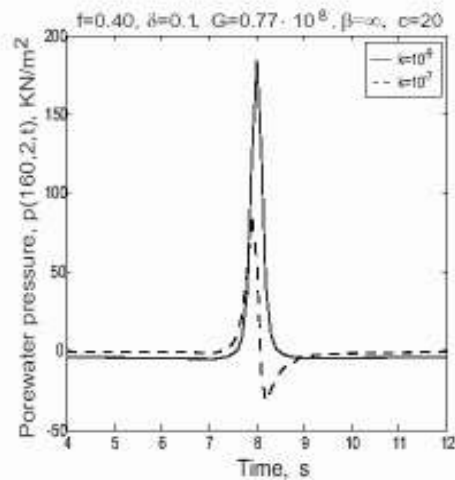


**Figure 5(a). Effect of permeability on porewater pressure at 2.0m depth varied with moving load position:  $c = 20 \text{ m/s}$**

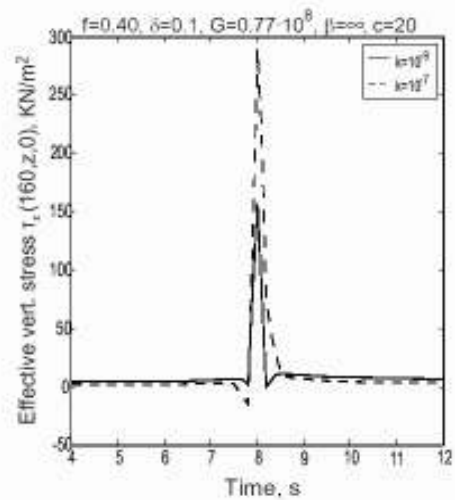


**Figure 5(b). Effect of permeability on effective vertical stress at 2.0m depth varied with moving load position:  $c = 20 \text{ m/s}$**

The effect of permeability on the pore water pressure and solid vertical effective stress generated at 2.0m depth as the moving load approaches the point of interest ( $x=160\text{m}$ ) is shown in Figures 5 (a) and (b) for  $c=20\text{m/s}$ . One can see that increasing permeability reduces considerably (of about 45%) the

peak water pressure and increases, as expected, the peak solid vertical effective stress since the fluid shares a smaller part of the applied load. However, for high speeds, each of the  $p$  and  $\tau_z$  responses (not shown here) for both permeabilities are of the same order of magnitude, since solid and fluid tend to move together and therefore the energy dissipated by the moving load, which is proportional to the difference of solid and fluid velocities, reduces drastically (Biot, 1956).

### APPROXIMATE APPROACH

This method of solution of the problem considered is based on the theory of Mei and Foda (1981), according to which the total field of a poroelastic problem in the frequency domain obeying Biot's (1956) theory can be approximated by the superposition of i) an elastodynamic problem with modified elastic constants and solid mass density for the whole domain (the outer approximation) and ii) a diffusion problem for the pore fluid pressure confined to a thin boundary layer at the free boundaries of the domain (the boundary layer correction). This implies that any total function  $\phi(x, z, t)$  of the system has the form:

$$\phi(x, z, t) = \phi^o(x, z, t) + \phi^b(x, z, t) \quad (19)$$

where the outer approximation and boundary layer correction functions are distinguished by the subscripts o and b, respectively.

#### The outer approximation

Referring to the outer region one can show that if  $R_n \gg f(\lambda_n c)H^2 / Gk$ , where the quantity  $\lambda_n c$  represents the parameter of frequency in the domain of Fourier expansion, then  $u^o = (u^f)^o$  and  $w^o = (w^f)^o$ , and Eqs (1), (2), (4) and (5) yield the expressions (Theodorakopoulos et al, 2003)

$$G^* \left( \frac{\partial^2 u^o}{\partial x^2} + \frac{\partial^2 u^o}{\partial z^2} \right) + (\lambda^* + G^* + \beta / f) \left( \frac{\partial^2 u^o}{\partial x^2} + \frac{\partial^2 w^o}{\partial x \partial z} \right) = [(1-f)\rho_s + f\rho_f] \ddot{u}^o \quad (20)$$

$$G^* \left( \frac{\partial^2 w^o}{\partial x^2} + \frac{\partial^2 w^o}{\partial z^2} \right) + (\lambda^* + G^* + \beta / f) \left( \frac{\partial^2 w^o}{\partial z^2} + \frac{\partial^2 u^o}{\partial x \partial z} \right) = [(1-f)\rho_s + f\rho_f] \ddot{w}^o \quad (21)$$

It is observed that Eqs (20) and (21) are the same as in classical elastodynamics for a simple phase medium but with new equivalent elastic constants and mass density of the form

$$G_e^* = G^*, \quad \lambda_e^* = \lambda^* + \beta / f, \quad \rho_e = (1-f)\rho_s + f\rho_f \quad (22)$$

The solution of the modified elastodynamic problem for the whole domain, which is governed by Eqs (20), (21) and (22), is obtained by a manner similar to that described in the previous section for the exact solution, and subject to the following four boundary conditions:

$$\text{At the bottom } (z=H): \quad w = w^o = 0, \quad u = u^o = 0$$

$$\text{At the surface } (z=0): \quad \tau_{xz} = \tau_{xz}^o = 0, \quad \tau_z = \tau_z^o + \tau_z^b = F \quad (23)$$

Details for the solution of the above system can be found in Theodorakopoulos et al (2003).

#### The boundary layer correction

Referring to Eqs (1), (2) and (3) and based on the arguments of Mei and Foda (1981), one can prove that (Theodorakopoulos et al, 2003)

$$k \frac{g^2 p^b}{g^2 z} - D \dot{p}^b = 0 \text{ with } D = \frac{f}{\beta} + \frac{1}{\lambda^* + 2G^*} \quad (24)$$

which is a heat diffusion equation that can be easily solved. Eq. (24) is the governing equation of the boundary layer for the pore fluid pressure  $p^b$ . It should be noted that this boundary layer formulation is only valid when the depth of the soil layer,  $H$ , is much higher than the boundary layer thickness,  $d_n$  for each harmonic. On the basis of Eq. (8) modified for  $p^b$ , Eq. (24) can be written as

$$(P_n^b)'' - \frac{(-i\lambda_n c)}{k} D P_n^b = 0 \quad (25)$$

The general solution of Eq. (25) is given by

$$P_n^b(z) = \Gamma_{1n} e^{sz} + \Gamma_{2n} e^{-sz} \quad (26)$$

in which the integration constants  $\Gamma_{1n}$  and  $\Gamma_{2n}$  may now be determined by employing the following boundary conditions

$$\begin{aligned} \text{At } z = d : \quad p^b &= 0 \\ \text{At } z = 0 : \quad p &= p^o + p^b = 0 \end{aligned} \quad (27)$$

These constants and the coefficient  $s$  can be found as functions of the quantity  $\lambda_n c$  elsewhere (Theodorakopoulos et al, 2003).

After the determination of the pore fluid pressure inside the boundary layer, one can find the vertical solid displacement  $w^b$  and the effective vertical solid stress  $\tau_z^b$ . For explicit expressions of these quantities, one can look at Theodorakopoulos et al (2003). Consequently, inside the boundary layer the expressions for the total  $w(x, z, t)$ ,  $p(x, z, t)$  and  $\tau_z(x, z, t)$  can be written as

$$\begin{aligned} w(x, z, t) &= Re \sum_0^{2048} (W_n^o + W_n^b) e^{i\lambda_n(x-ct)} \quad \text{for } 0 \leq z \leq d_n \\ p(x, z, t) &= Re \sum_0^{2048} (P_n^o + P_n^b) e^{i\lambda_n(x-ct)} \quad \text{for } 0 \leq z \leq d_n \\ \tau_{z,n}(x, z, t) &= Re \sum_0^{2048} (T_{z,n}^o + T_{z,n}^b) e^{i\lambda_n(x-ct)} \quad \text{for } 0 \leq z \leq d_n \end{aligned}$$

## Numerical results and discussion

### *The boundary layer correction contribution*

To apply the approximate (superposition) approach to the solution of the problem considered one should first ensure the validity of  $H/d_n \gg 1$ , for various combinations of the parameters  $f$ ,  $\lambda_n c$ ,  $k$  and  $G$ . Figures 6 (a) and (b) show the effect of adding the contribution of the boundary layer correction to the outer approximation response, for the maximum vertical displacement, which is of main interest for engineers, for two values of permeability  $k$ ,  $G = 10^8 \text{ N/m}^2$  and a specific value of load velocity in each figure. It should be noted that the outer approximation solution is independent of the value of  $k$  (Theodorakopoulos et al, 2003). From Figure 6 it can be seen that for both values of load velocity, the effect of boundary layer correction is a small percentage of the total response and increases with increasing permeability.



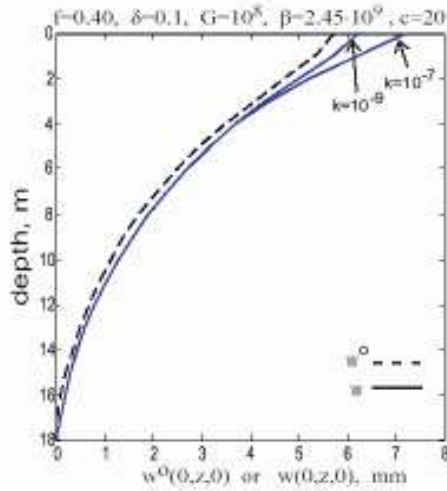


**Figure 6(a). Effect of the boundary layer correction on maximum solid vertical displacement versus depth,  $c=20$  m/s**

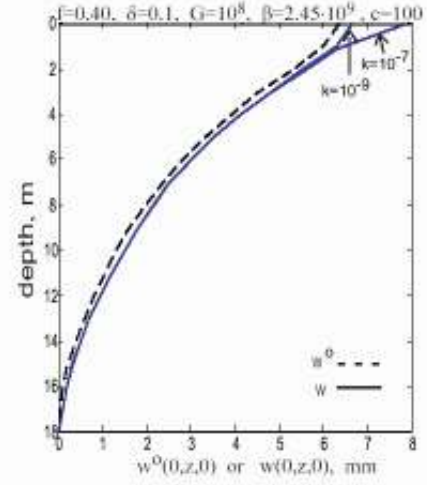


**Figure 6(b). Effect of the boundary layer correction on maximum solid vertical displacement versus depth,  $c=100$  m/s**

Thus, one can conclude that for soils with low permeability,  $k = 10^{-9} \text{ m}^3/\text{s}/\text{kg} = 10^{-5} \text{ m/s}$ , the outer approximation response, being of about 94% of the total response, may be the only contributor to the displacement response for engineering purposes. Furthermore, for soils with low permeability, similar conclusions can be drawn for the pore water pressure and vertical effective stress, as found in Theodorakopoulos et al (2003).

#### *Comparison between approximate method and exact solution*

Figures 7 (a) and (b) show the variation with depth of the vertical displacement and porewater pressure, respectively, according to both the present approximate method and the exact solution for  $G = 10^8 \text{ N/m}^2$ ,  $k=10^{-9} \text{ m}^3/\text{s}/\text{kg}=10^{-5} \text{ m/s}$  and for two values of load velocity  $c$  (20, 100 m/s) in each figure. It can be seen that the agreement between the two solutions is very satisfactory for both response functions. These conclusions are the consequence of the fact that in the case of a fine material ( $k=10^{-9} \text{ m}^3/\text{s}/\text{kg}=10^{-5} \text{ m/s}$ ) the values of  $R_{n=1}$  and  $H/d_{n=1}$  are much larger than unity, as required by the theory of Mei and Foda (1981). Furthermore, it is observed from Figures 7 (a) - (b), that for  $c=100 \text{ m/s}$ , the agreement between the two solutions is even more satisfactory due to the even more larger values of the quantities  $R_{n=1}$  and  $H/d_{n=1}$  computed in this case.

The comparison of the response of the soil medium under moving loads between the approximate method and the exact solution for the case of a coarse material ( $k=10^{-7} \text{ m}^3/\text{s}/\text{kg}=10^{-3} \text{ m/s}$ ), is shown in Figures 8 (a) and (b), again for two values of load velocity  $c$  (20, 100 m/s) in each figure. One can see that the agreement between the two solutions, as far as the vertical displacement is concerned, Figure 8 (a), is yet excellent, although for the coarse material the depth of the boundary layer  $d_{n=1}$  is not small compared to the layer depth  $H$ . However, it can be observed that there is a discrepancy between the two solutions for the pore water pressure, Figure 8 (b). This may be attributed to the large depth of the boundary layer,  $d_{n=1}$ , which seems to affect the distribution of the applied load between solid and fluid more than it affects the overall response of the vertical displacement when the approximate method is used. It should be reminded that the value of the ratio  $H/d_{n=1}$  increases proportionally to the square root of  $c$ , and this explains the smaller discrepancies in  $p$  between the two solutions when the load velocity increases from  $c = 20 \text{ m/s}$  to  $c = 100 \text{ m/s}$ , respectively, as shown in Figure 8 (b).

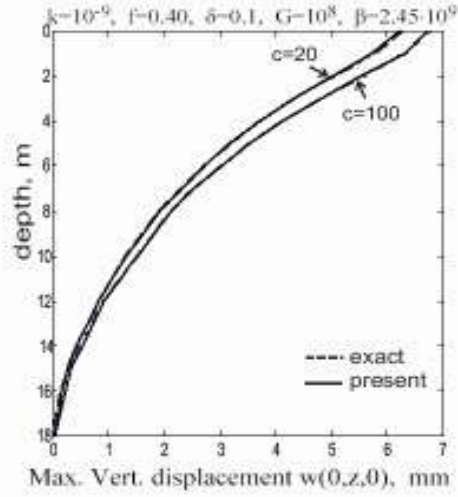


Figure 7(a). Comparison of the maximum vertical displacement between the approximate method and exact solution,  $k=10^{-9} \text{ m}^3/\text{kg}=10^{-5} \text{ m/s}$ ,  $G=10^8 \text{ N/m}^2$

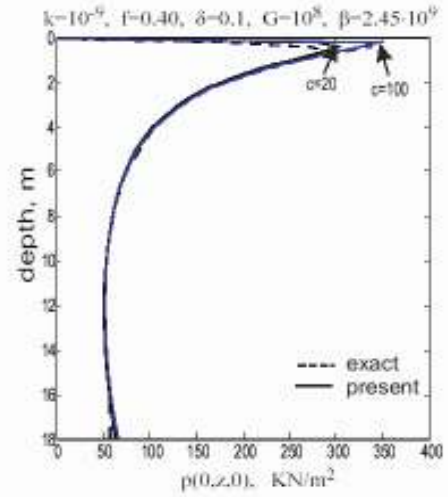


Figure 7(b). Comparison of porewater pressure between the approximate method and exact solution,  $k=10^{-9} \text{ m}^3/\text{kg}=10^{-5} \text{ m/s}$ ,  $G=10^8 \text{ N/m}^2$

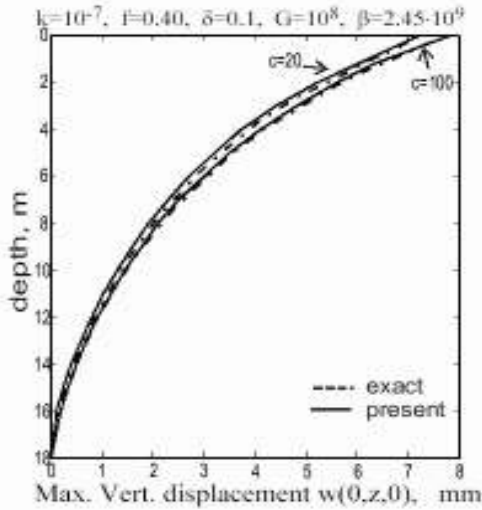


Figure 8(a). Comparison of the maximum vertical displacement between the approximate method and exact solution,  $k=10^{-7} \text{ m}^3/\text{kg}=10^{-3} \text{ m/s}$ ,  $G=10^8 \text{ N/m}^2$

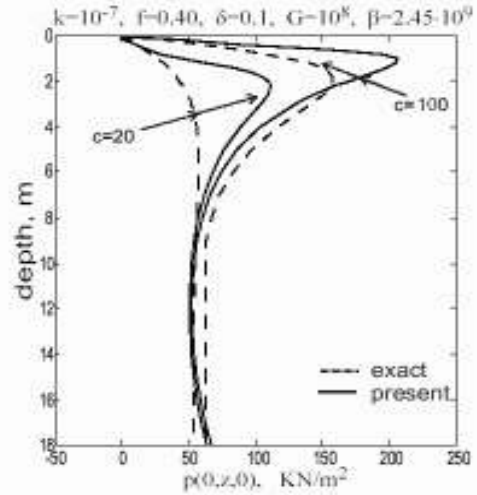


Figure 8(b). Comparison of porewater pressure between the approximate method and exact solution,  $k=10^{-7} \text{ m}^3/\text{kg}=10^{-3} \text{ m/s}$ ,  $G=10^8 \text{ N/m}^2$

## CONCLUSIONS

On the basis of the results presented in this paper and additional results not shown here (Theodorakopoulos, 2003, Theodorakopoulos et al, 2003) the following conclusions can be drawn:

1. The governing partial differential equations for the poroelastic soil medium under the action of a strip moving load were derived and the expressions for the pore water pressure and the vertical solid

skeleton displacements and stresses were determined by both an exact and an approximate solution approach.

2. Parametric studies show that the vertical displacement increases with decreasing values of fluid compressibility and shear modulus and with increasing values of permeability. The dynamic effect of increasing load velocity is almost independent of the shear modulus, with the other material properties being kept constant.

3. In the framework of the approximate solution, the effect of the boundary layer correction on the response is nearly negligible, especially for the case of a soil material with low permeability.

4. The numerical results of the approximate solution are very well compared with those of the exact solution and, therefore, the approximate method provides an alternative method of analysis, especially in the case of fine materials.

## REFERENCES

- Biot, M. A., 1956. Theory of Propagation of Elastic Waves in a Fluid-Saturated Porous Solid. Part I: Low-Frequency Range; Part II: High-Frequency Range, *Journal of the Acoustical Society of America*, 28: 168-191.
- Foda, M. A., Mei, C. C., 1983. A Boundary Layer Theory for Rayleigh Waves in a Porous Fluid-Filled Half-Space, *Soil Dynamics and Earthquake Engineering*, 2: 62-65.
- Mei, C. C., Foda, M. A., 1981. Wave-Induced Responses in a Fluid-Filled Poroelastic Solid with a Free Surface—a Boundary Layer Theory, *Geophysical Journal of the Royal Astronomical Society*, 66: 597-631.
- Theodorakopoulos, D. D., 2003. Dynamic Analysis of a Poroelastic Half-Plane Soil Medium under Moving Loads, *Soil Dynamics and Earthquake Engineering*, 23: 521-533.
- Theodorakopoulos, D. D., Chassiakos, A. P., Beskos, D. E., 2003. Dynamic Effects of Moving Load on a Poroelastic Soil Medium by an Approximate Method, *International Journal of Solids and Structures*, in press.